26th International Congress on Sound and Vibration
7-11 July 2019, Montreal

FULL-SCALE CABIN NOISE FROM TURBULENT BOUNDARY LAYER EXCITATION, PART 1 : WALL-PRESSURE MEASUREMENT AND ANALYSIS

Simon L. Prigent, Édouard Salze, Emmanuel Jondeau and Christophe Bailly.
Univ Lyon, École Centrale de Lyon and LMFA UMR CNRS 5509, Ecully, France.
email: simon.prigent@ec-lyon.fr

Romain Leneveu.
VibraTec, Ecully, France.

The present paper is part of a two-fold study focused on cabin noise conducted within the frame of the Canoble project of the EU's CleanSky2 programme. The turbulent boundary layer developing on the fuselage creates excitation through wall pressure fluctuations that are, to some extent, transmitted and radiated inside the cabin, contributing to a significant part of the noise during cruise. Many studies have looked into the properties and structures of wall pressure fluctuations beneath a turbulent boundary layer, however there is still a lack of knowledge for some of their components and on the effect of pressure gradients, more so on realistic geometries. Hot-wires and hot-films have been used to characterise the boundary layer while newly developed antennas of digital MEMS microphones served for the measurement of wall pressure. The latter technology had previously been tested in duct flow by some of the authors and was able to isolate acoustic components from the hydrodynamic ones. The microphones themselves are embedded into a circuit board which reduces the overall thickness to only a few millimetres, and enables the measurements to be carried out without intrusive modification of the fuselage. Such an approach opens the door to in-flight tests in the future. These measurements have been performed on a scale-one mock-up of the fore part of a Dassault Aviation business jet, in an industrial-size wind tunnel. The boundary layer parameters along with the wall pressure spectra that were successfully measured will serve as inputs for the second part focusing on vibrational behaviour and noise radiation inside the cabin.
Keywords: aero-acoustics, wall pressure, interior noise.

1. Introduction

The characterisation of wall pressure fluctuations beneath a turbulent boundary layer has captivated the attention of researchers during several decades [1]. Such fluctuations can cause structural vibrations and in turn radiate noise through a wall which is the cause of cabin noise, or cause damage to the load of a rocket in a more extreme case. Underwater, these fluctuations can pollute the signal received by a sonar system. While a fair understanding - although still suffering from a scatter of experimental data [2] - has been reached for the simple case of a flat plate with zero-pressure gradient, power spectra of such fluctuations are poorly known under mean pressure gradient conditions. Naturally, industrial applications often involve complex geometries that generate such conditions. Moreover, the power spectra themselves are not enough to characterise the fluctuations and the wavenumber - frequency spectra are needed to better understand how these vibrations can radiate through a structure. The present study focuses on wall pressure fluctuations, from their characterisation in terms of wavenumber - frequency spectra to the study of their acoustic radiation in the cabin, by means of experimental measurements on a full-scale mock-up. The vibration and radiation aspects will be addressed in a companion paper [3], while this paper focuses on the characterisation of the turbulent boundary layer itself and the discussed spectra and other relevant physical quantities describing the spatio-temporal structure of the fluctuations.

2. Experimental approach & apparatus

2.1 Wind-tunnel and mock-up

Measurements are conducted in the S2A industrial aeroacoustic wind tunnel near Paris, France. The closed-loop tunnel opens to a test room with an inlet section of $24\,\mathrm{m}^2$. The test room itself is $15\,\mathrm{m}$ long and its walls are treated against acoustic reverberation. An outlet (seen in black in fig. 1) then guides the air back into the loop. Results presented in this paper have been measured with outer velocities ranging from 15 to $65\,\mathrm{m.s}^{-1}$.

The mock-up used in this study is a full-scale fore part of a Dassault Aviation business jet. The mock-up is $10\,\mathrm{m}$ long in total, with the first $6\,\mathrm{m}$ true to the aeroplane geometry, and the remainder serving as a tail to streamline the rear end. The outer surface was milled to the geometry while static pressure sensors were fitted along some specific streamlines and two kinds of inserts were added. First, panels mimicking the vibrational behaviour of a real jet fuselage were added to the structure, and were equipped with accelerometers to study noise radiation. This latter topic will be addressed by the Part 2 of this study. Second, modules supporting wall pressure microphone antennas, hot films, hot wires and other devices were placed in locations mirroring those of the panels. Those three modules correspond, respectively, to the roof, windscreen and side panel. Finally, the inside of the mock-up was hollowed to store electronics and allow for interior noise measurements.

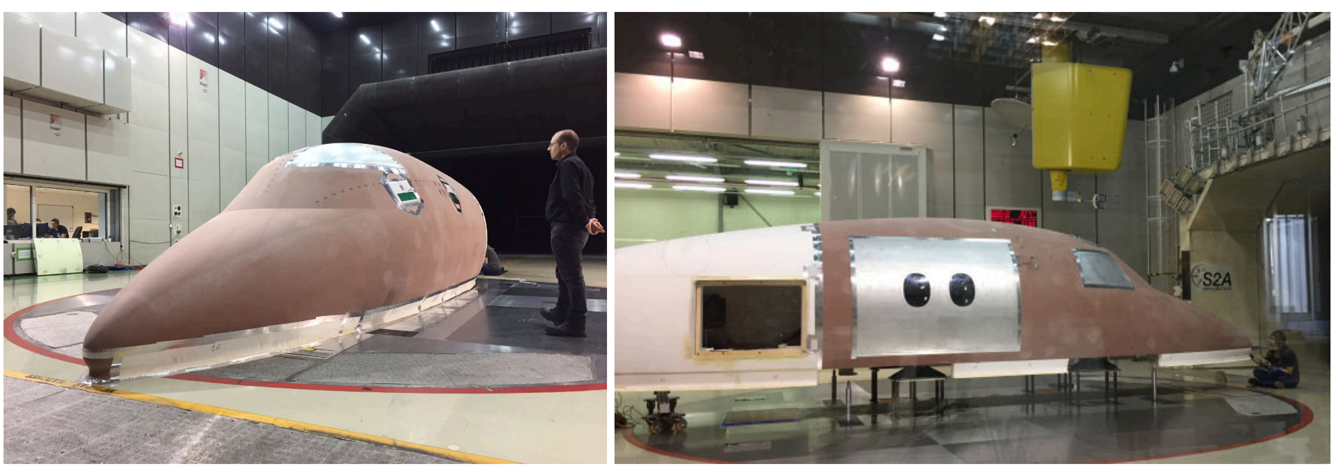

Figure 1: Mock-up installed in the wind tunnel.

2.2 Antenna

Previous studies by some of the present authors have looked into the possibility to measure wavenumber - frequency spectra of wall pressure fluctuations with a rotating line array of remote microphones [4, 2, 5, 6]. The remote approach has proven useful and offers the clear advantage of reducing the spacing between measurement locations and to fit the remote tubes with anechoic ends to avoid resonance. The antenna's rotation also provides an increased number of separation vectors in the physical space that in turn increases the accuracy of the space - Fourier transform. However, in its current state, this technology requires back access through the studied wall, and is only suited to a laboratory wind tunnel where a wall can be fitted with such a system.

In the current study, non-intrusiveness was a key feature, keeping in mind future developments where the developed antennas would be fitted onto real aerocrafts for which any intrusive approach is out of the discussion. Some recent studies have shown the possible use of MEMS microphones for wall pressure measurements [7, 8], and was shown to enable the separation of acoustic and hydrodynamic components of the fluctuations which in turns lead to modal analysis said acoustic part. The present antenna is thus based on the array presented by Salze *et al.* [8]. The distribution of the microphones on the board is illustrated in fig. 4.

Each antenna is composed of 40 digital microphones, non-uniformly distributed on a cross whose main axis is aligned with the flow direction. The microphones themselves are InvenSense's $4 \times 3 \times 1$ mm^3 INMP621 digital microphones which output digital data. The reader is referred to the study by Salze *et al.* [8] for further details on the digital architecture (clock generation, digital bus decoding etc.) of such an array. During each measurement run, data is sampled at $50\,\text{kHz}$ during $60\,\text{s}$.

The electronic board on which the microphones are affixed is flush-mounted onto a mask that is fitted to the outer geometry of the fuselage. The total added thickness is of $2.5\,\text{mm}$. Tests have been carried out in the acoustic wind tunnel at Ecole Centrale de Lyon, both with and without mask to assess the effect of the added thickness and the robustness of the technology at the targetted velocities.

2.3 Boundary layer measurement

The modules supporting the antenna were fitted with a reference microphone and a hot film, and enabled a traverse to be installed for hot-wire measurements. The boundary layer was thus characterised for each target velocity and the friction velocities obtained from fitted profiles were satisfactorily checked against those directly measured with hot films. The mean velocity profiles, normalised by wall units and obtained for the three modules, are shown in fig. 2 for three representative outer velocities: 30, 45 and 65 m.s^{-1}.

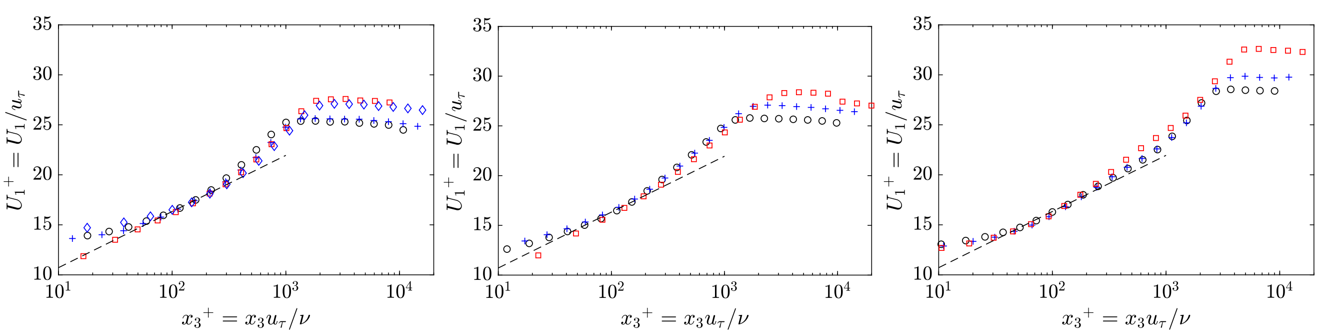

Figure 2: Mean profiles in wall units for the three modules, ordered from left to right, at 30 (circles), 45 (pluses) and 65 m.s^{-1} (squares). Extra velocity for module 1 at 70 m.s^{-1} (diamonds).

The boundary layers from modules 1 and 2 exhibit very similar profiles, reaching almost the same values and starting their plateau at the same normalised distance from the wall. On the other hand, the profiles from module 3 reach higher values of normalised velocity and the logarithmic region is more developed. This is in fact expected, as module 1 and 2 are placed in similar positions in terms of distance from the nose, and both displacement thickness and friction velocities are found to be very close between the two modules. Module 3 mirrors the side panel and is therefore further downstream, which explains the more developed logarithmic region. The higher values of U_1^+ are due to a lower friction velocity, for instance, at 30 m.s^{-1}, u_τ is measured at 1.3 m.s^{-1} for modules 1 and 2, and 1.1 m.s^{-1} for module 3.

In addition, 64 static pressure (P) probes were placed alongside streamlines that had been selected to cross the measurements location, to directly measure the local pressure gradient. The non-dimensional pressure gradient parameter, or Clauser parameter, $\beta = (\delta_1/\tau_w)\nabla P$ for the three modules at 30 m.s^{-1} is 0.03, -0.15 and 0.08, respectively. At 45 m.s^{-1}, the same parameters are 0.053, -0.22 and 0.11, respectively. This indicates that the boundary layer over module 1 is subjected to an almost-zero pressure gradient, the one over module 2 to a favourable pressure gradient, and the one over module 3 to a mild adverse one.

3. Spectra

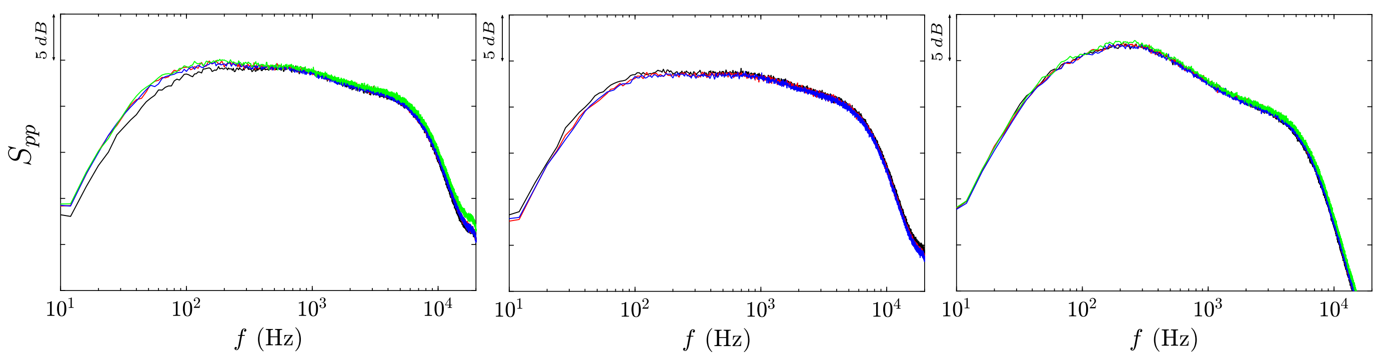

Figure 3: Pressure spectra for the three modules, ordered from left to right, at 30 m.s^{-1}

The goal of this measurement campaign is to obtain the physical quantities that are necessary to the simulation of structure vibration and in turn noise radiation. The initial step is to measure the intensity of the excitation from wall pressure fluctuations.

Given that such measurements are run at different times to accommodate for various configurations, it is important to ensure a good repeatability of the measurements. The spectra obtained for the same target velocity (30 m.s^{-1}) but at different times, and even after moving the mock-up out of the wind tunnel and installing it back again, are presented in fig. 3 for the three antennas. It is clear that all measurements are close to identical, which speaks in favour of the reliability of the measurements and the comparison between data from different sessions.

Comparing the spectra at different locations, one notices that the ones from module 3 have an increased content at frequencies around $100 - 1000$ Hz while the two others are rather flat. As previously mentioned, the velocity profiles on module 1 and 2 are very similar, so it is not surprising that the spectra should be similar too. The shape of the spectra is in fact similar to what can be found in turbulent boundary layers under a zero- or favourable static pressure gradient, which corresponds to the values of

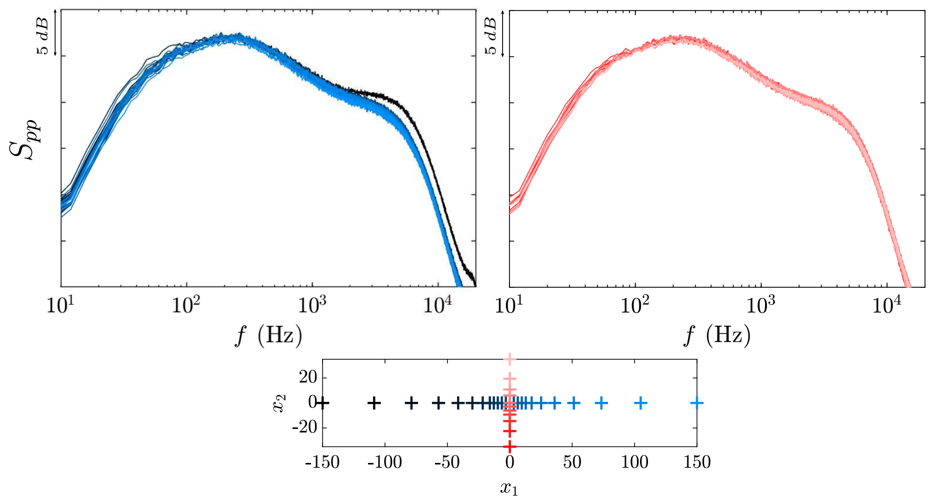

Figure 4: Pressure spectra from all microphones of module 3 at 30 m.s^{-1}, along the longitudinal (left) and transverse (right) lines. Positions of the corresponding microphones on the board (bottom).

β (0.03 and -0.15) previously discussed. On the other hand, a mildly adverse pressure gradient was measured over module 3 ($\beta = 0.08$), and the corresponding spectra have the expected shape for this pressure gradient condition.

The power spectral density of all microphones from the antenna mirroring the panel are displayed in fig. 4. An emphasis is put on this module as it corresponds to the panel that is fitted with accelerometers, and hence allow the most comprehensive vibration and radiation study. Apart from one of the microphone that slightly deviates at high frequencies, all spectra collapse which shows a good homogeneity of the flow over the antenna. Such homogeneity is an important requirement to perform Fourier transforms in order to compute the wavenumber-frequency spectra, as illustrated later on.

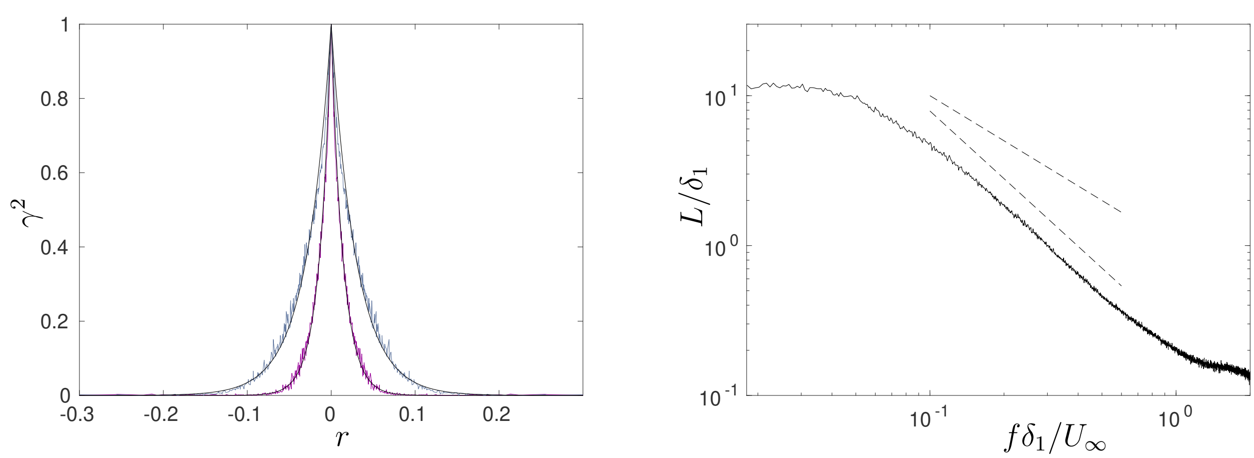

Figure 5: Stream-wise coherence with exponential decay at 400 Hz and 800 Hz for module 3 at 30 m.s^{-1} (left), and corresponding coherence scale.

Indeed, the intensity of the excitation alone does not provide a sufficient description, and its spatial structure is also needed. Fig. 5 shows the stream-wise coherence on module 3 at 30 m.s^{-1}, at two frequencies, and an exponential decay fit. Fitting such a decay at each frequency gives the stream-wise (or longitudinal) coherence scale that is displayed in the same figure, with both -1 and $-3/2$ power laws for reference.

4. Wavenumber-frequency spectra

Another, comprehensive, description of both spatial and temporal structures of the fluctuations is the computation of the wavenumber-frequency spectra. It is, by definition, the Fourier transform of the spatio-temporal correlation function, and is in practice evaluated by Fourier transforming in space the cross-spectra.

Fig. 6 shows the one dimensional wavenumber-frequency spectra for various velocities at the location mirroring that of the side panel. The acoustic wavenumber and the convective one, defined as $k_c = 2\pi f/(0.8 \times U_\infty)$ are added for reference at 30 and 45 m.s^{-1}. The convective ridge is clearly visible on the $k_1 - f$ maps, however, no acoustic component can be found. Some artefacts are visible at low frequencies, up to $500\,$Hz for the highest velocities, that are most likely due to the discretisation of the antenna. Apart from this aspect, the maps are overall clearly measured, which shall be helpful in using them for interior noise applications. Similar results had been obtained by the authors in a preliminary design phase of the technology, but in research facilities with a channel flow at the Centre Acoustique of Ecole Centrale de Lyon [8]. It is thus encouraging to see that despite the difficulties added by this realistic aeroplane geometry, the matured technology has proven reliable.

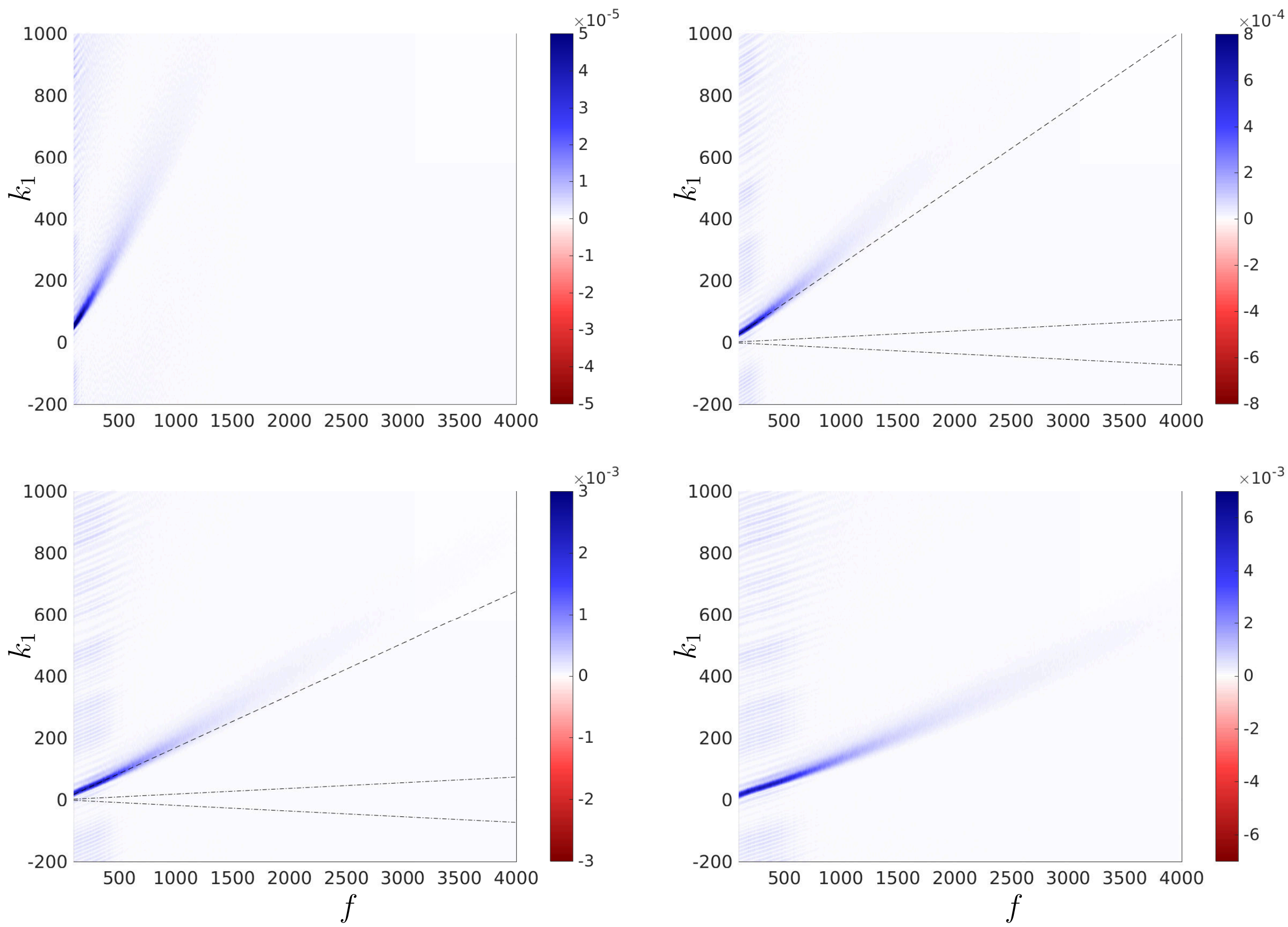

Figure 6: $k_1 - f$ maps of spectrum for (from top left to bottom right) 15, 30, 45 and 60 m.s^{-1}.

For reference, one-dimensional spectra from the two other modules are presented in fig. 7. The acoustic wavenumber and the convective one, defined as $k_c = 2\pi f/(0.8 \times U_\infty)$ are again added for reference. These spectra are rather similar, in terms of levels and structures, which corroborates the previous observations that both modules are measuring similar boundary layers. They do, however, have lower levels than that of module 3 at the same velocity, and their associated convection velocity is lower. This is in fact logical, since pressure spectra already exhibited lower levels, and the mean velocity profiles had shown lower values.

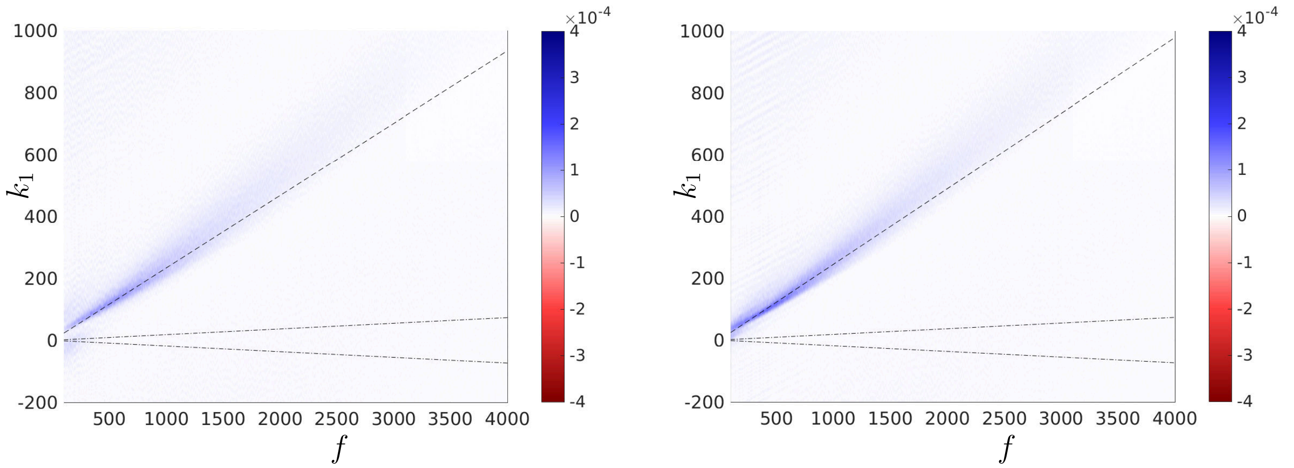

Figure 7: $k_1 - f$ maps of spectrum for modules 1 (left) and 2 (right) at 30 m.s^{-1}.

5. Concluding remarks

The experimental campaign presented in this paper was conducted on a full-scale mock-up of a business jet. It has provided boundary layer parameters such as friction velocities and displacement thickness alongside velocity profiles, at key measurement locations. Thanks to recently developed technology, further analysis has then been conducted in terms of spectra and wavenumber-frequency spectra of wall pressure fluctuations, to allow for a comprehensive spatio-temporal characterisation of said fluctuations. Combining those results not only offers an insight into the physics at stake in such an industrial configuration, it also enables the modelling and computation of structure vibration under the excitation of the boundary layer. The latter aspect is the topic of the second part of this two-fold study.

Acknowledgement

This research has been funded by the European Union through the CANOBLE Cleansky project (H2020-CS2-CFP02-2015-01, project id 717084), and by the Labex CeLyA of Université de Lyon, operated by the French National Research Agency (ANR-10-LABX-0060/ ANR-11-IDEX-0007).

REFERENCES

1. Bull, M. K. Wall-pressure fluctuations beneath turbulent boundary layers: some reflections on forty years of research. *Journal of Sound and vibration*, 190(3), 299-315, (1996).

2. Salze, E., Bailly, C., Marsden, O., Jondeau, E. and Juvé, D. An experimental characterisation of wall pressure wavevector-frequency spectra in the presence of pressure gradients. *20th AIAA/CEAS Aeroacoustics Conference* (p. 2909), (2014).

3. Leneveu, R., Rissmann, M., Alonso, A. and Salze, E. Full-scale cabin noise from turbulent boundary layer excitation, part 2: vibroacoustic modelling and transmission. *26th international congress on sound and vibration*. (2019).

4. Arguillat, B., Ricot, D., Bailly, C. and Robert, G. Measured wavenumber - frequency spectrum associated with acoustic and aerodynamic wall pressure fluctuations. *American Institute of Aeronautics and Astronautics Journal*. 128(4),1647-1655, (2010).

5. Salze, E., Bailly, C., Marsden, O., Jondeau, E., and Juvé, D. An experimental investigation of wall pressure fluctuations beneath pressure gradients. *21st AIAA/CEAS Aeroacoustics Conference* (p. 3148), (2015).

6. Prigent, S. L., Salze, E. and Bailly, C. Deconvolution of the wavenumber - frequency spectra of wall pressure fluctuations. *American Institute of Aeronautics and Astronautics Journal*. under review.

7. Bremner, P., Todter, C., and Clifton, S. Sideglass turbulence and wind noise sources measured with a high resolution surface pressure array. *SAE International Journal of Passenger Cars-Mechanical Systems*, 8(2015-01-2325), 1063-1074, (2015).

8. Salze, E., Jondeau, E., Pereira, A., Prigent, S. L. and Bailly, C. A new MEMS microphone array for the wavenumber analysis of wall-pressure fluctuations: application to the modal investigation of a ducted low-Mach number stage. *25th AIAA/CEAS Aeroacoustics Conference*.(2019) .